

Multifocal Sparganosis Mimicking Lymphoma Involvement: Multimodal Imaging Findings of Ultrasonography, CT, MRI, and Positron Emission Tomography-Computed Tomography

림프종으로 오인된 다발성 스파르가눔증: 초음파, 전산화단층촬영, 자기공명영상, 양전자단층촬영의 다양한 영상 소견

So Young Heo, MD¹, Ji Yeon Park, MD^{1*}, Noh Hyuck Park, MD¹, Chan Sub Park, MD¹,
Taejung Kwon, MD², Seong Yoon Yi, MD³, Hyun Jung Jun, MD⁴

Departments of ¹Radiology, ²Pathology, Myongji Hospital, Seonam University College of Medicine, Goyang, Korea

³Division of Hematology-Oncology, Department of Internal Medicine, Inje University Ilsan Paik Hospital, Goyang, Korea

⁴Division of Hematology-Oncology, Department of Internal Medicine, Seoul Medical Center, Seoul, Korea

Sparganosis is a rare parasitic disease caused by the migrating plerocercoid larva of *Spirometra* species tapeworms. The most frequent clinical manifestation is a subcutaneous nodule resembling a neoplasm. In this study, we presented multimodal findings of ultrasonography, computed tomography, magnetic resonance imaging, positron emission tomography-computed tomography and follow-up imagings on multifocal sparganosis, mimicking lymphoma involvement in a patient with lymphoma.

Index terms

Sparganosis
Diffuse Large B-Cell Lymphoma
Ultrasonography
CT
MRI
Positron Emission Tomography-Computed Tomography

Received March 18, 2015

Revised May 22, 2015

Accepted July 21, 2015

*Corresponding author: Ji Yeon Park, MD
Department of Radiology, Myongji Hospital,
Seonam University College of Medicine, 55 Hwasu-ro
14beon-gil, Deogyang-gu, Goyang 10475, Korea.
Tel. 82-31-810-6899 Fax. 82-31-810-6537
E-mail: zzzz3@hanmail.net

This is an Open Access article distributed under the terms of the Creative Commons Attribution Non-Commercial License (<http://creativecommons.org/licenses/by-nc/3.0>) which permits unrestricted non-commercial use, distribution, and reproduction in any medium, provided the original work is properly cited.

INTRODUCTION

Sparganosis is a rare parasitic infection caused by the plerocercoid of the cestode *Spirometra mansoni*. The definitive hosts are dogs and cats, and humans are typically infected as aberrant hosts. The clinical manifestations are diverse and the most common symptom presents as movable or fixed subcutaneous nodules. Differentiation of sparganosis from a soft tissue tumor and subcutaneous or skin metastasis in a patient with cancer is difficult; and imaging finding of sparganosis in lymphoma patient has rarely been reported (1, 2).

We reported multimodal image findings including ultraso-

nography (US), computed tomography (CT), magnetic resonance imaging (MRI), positron emission tomography-computed tomography (PET-CT) and follow-up imagings on multifocal sparganosis, mimicking lymphoma involvement in a patient with lymphoma.

This case was approved by the Institutional Review Board and informed consent was waived.

CASE REPORT

A 63-year-old man presented with a 1-month history of a palpable mass in the right medial thigh. He had experienced ne-

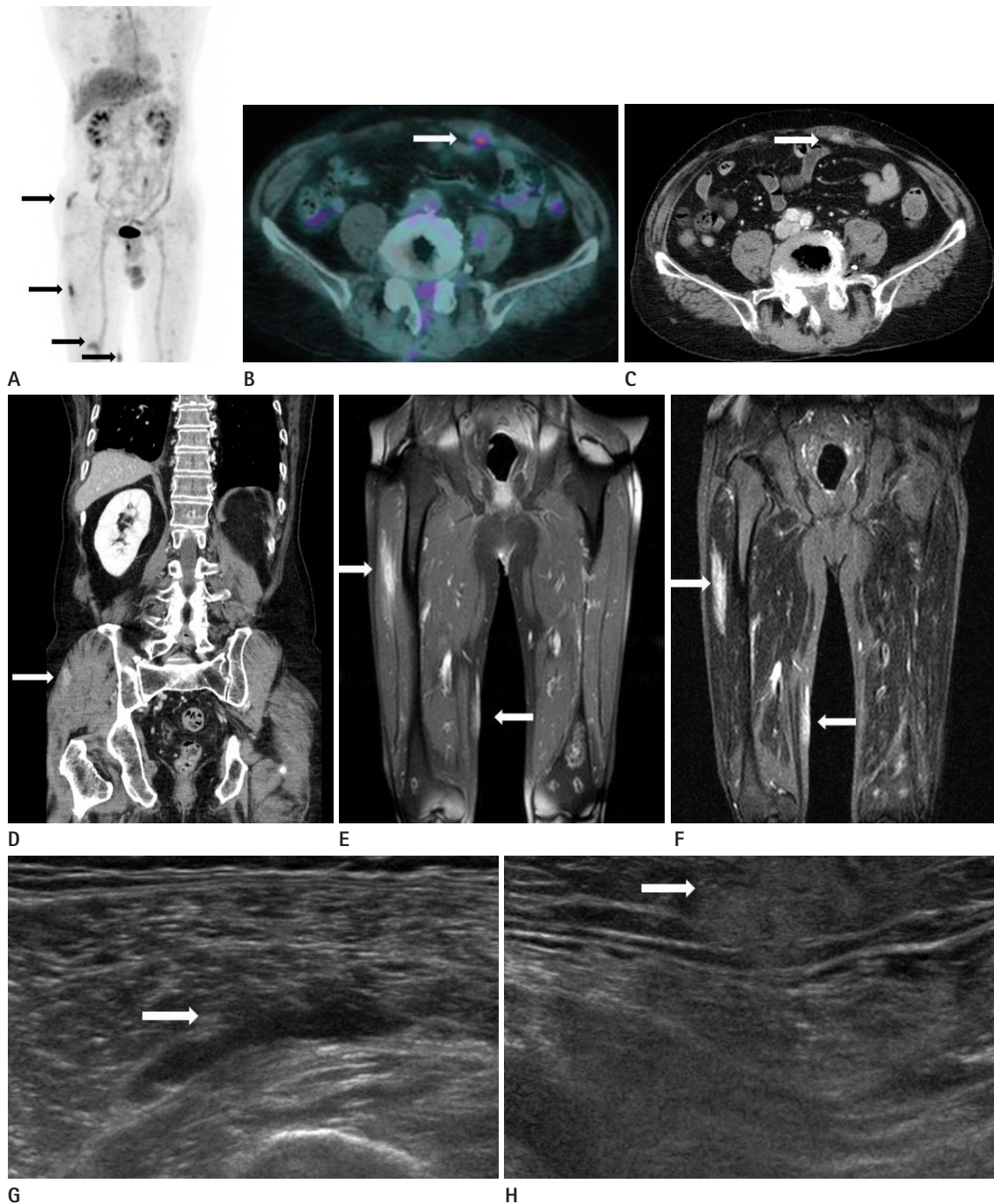


Fig. 1. PET-CT, abdomen CT, femur MRI and US images after 3 cycles of R-CHOP.

A, B. PET-CT reveals multiple hypermetabolic lesions (SUV = 3.6–5.2) with tubular shape in the right buttock, vastus lateralis muscle, medial thigh (**A**, black arrows) and left rectus abdominis (**B**, white arrow).

C, D. Abdomen CT shows ill-defined peripheral rim enhancing lesions with central low attenuation in the left rectus abdominis (**C**, white arrow) and right gluteus muscle (**D**, white arrow).

E, F. Femur MRI shows peripherally enhancing tubular lesion in the right vastus lateralis muscle and homogeneous enhancing elongated lesion in the subcutaneous layer of the right medial thigh (**E**, white arrows). The lesions shows high signal intensity on STIR image (**F**, white arrows).

G, H. US reveals a hypoechoic lesion with tubular shape in the right vastus lateralis (**G**, white arrow) and a heterogeneous hyperechoic lesion with ill-defined margin in the subcutaneous layer of the medial thigh (**H**, white arrow).

CT = computed tomography, MRI = magnetic resonance imaging, PET-CT = positron emission tomography-computed tomography, R-CHOP = rituximab, cyclophosphamide, hydroxydaunorubicin (doxorubicin), oncovin (vincristine), prednisone, STIR = short tau inversion recovery, SUV = standardized uptake value, US = ultrasonography

phrotic syndrome 2 years earlier and was treated with glucocorticoid. Thereafter, he was incidentally diagnosed with diffuse large B-cell lymphoma in the right intercostal muscle and diaphragm, in the course of decortication for a chronic empyema.

After 3 cycles of R-CHOP (rituximab, cyclophosphamide, doxorubicin, vincristine, prednisolone), an approximately 2 × 2 cm hard and non-movable subcutaneous mass without pain was found in the right thigh. PET-CT revealed multiple hypermetabolic lesions in the right buttock, lateral thigh, medial thigh and left rectus abdominis [standardized uptake value (SUV) = 3.6–5.2] (Fig. 1A, B). Abdomen CT and femur MRI were subsequently performed. Abdomen CT revealed ill-defined peripherally enhancing lesions with central low attenuation in the right gluteus maximus, vastus lateralis and left rectus abdominis muscle (Fig. 1C, D). Femur MRI showed the tubular lesions with elongated tubular tracts of iso-signal intensity with peripheral enhancement on the T1-weighted image; on short tau inversion

recovery image, there was high signal intensity in the right vastus lateralis, popliteus muscle and subcutaneous layer of the right medial thigh (Fig. 1E, F). US for core-needle biopsy showed a hypoechoic tubular lesion in the right vastus lateralis muscle and a heterogeneous hyperechoic lesion in the subcutaneous layer of the right medial thigh (Fig. 1G, H). These multiple lesions were initially suspected as lymphoma involvement. US-guided 18 G core-needle biopsy was performed at the superficial lesion of the right medial thigh and intramuscular lesion in the right vastus lateralis. The pathologic diagnosis was chronic granulomatous inflammation with calcified materials but no evidence of malignancy. These findings were indicative of parasite. The laboratory results revealed white blood cell count (WBC) of $3.2 \times 10^3/\mu\text{L}$ without eosinophilia. An IgG antibody test for *Cysticercus*, *Sparganum*, *Paragonimus*, and *Clonorchis* was negative.

Two weeks later, he revisited our hospital for 4 cycles of chemotherapy and presented with a new palpable mass in the left

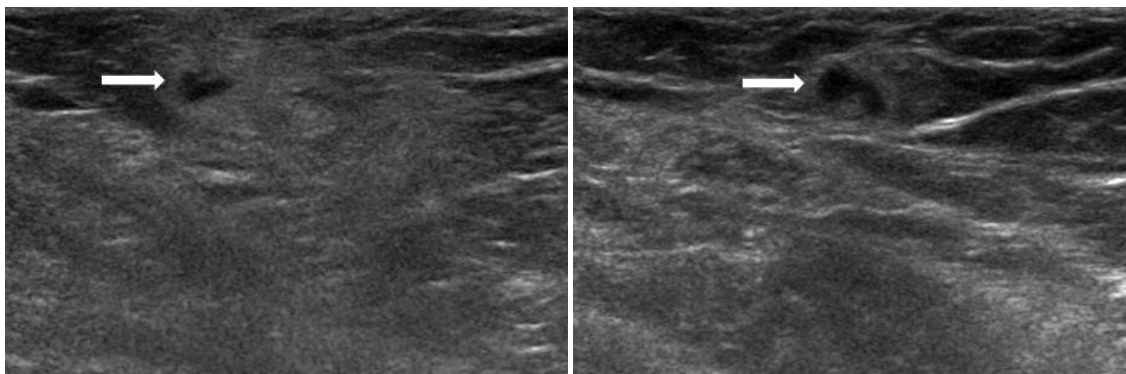


Fig. 2. Follow-up US after 2 weeks. US reveals a new, approximately 2.7 × 1.2 cm ill-defined hyperechoic lesion with internal small tubular hypoechoic area (white arrows) in the subcutaneous layer of left perineum. US = ultrasonography

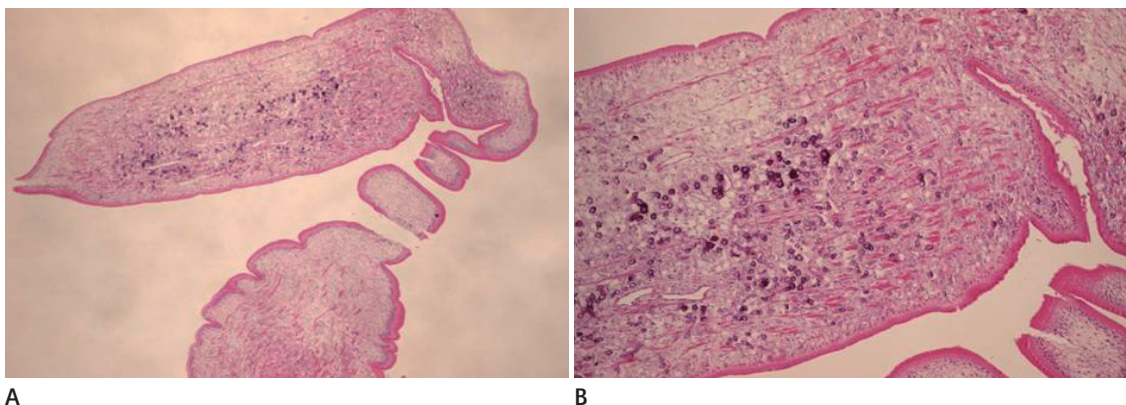


Fig. 3. Histopathologic examination of the right medial thigh. **A.** The sparganum shows eosinophilic folded tegument, subtegumental muscle fibers and calcospherules (hematoxylin-eosin, × 40). **B.** Higher magnification of the sparganum in **A.** The tegument is thick and muscle fibers are oriented longitudinally (hematoxylin-eosin, × 100).

inguinal area with tenderness. The laboratory findings included WBC count of $17.5 \times 10^3/\mu\text{L}$ with 1% eosinophils. A follow-up US revealed an approximate 2.7×1.2 cm hyperechoic lesion with an internal tubular hypoechoic tract in the superficial layer of the left perineum (Fig. 2) and the previous lesions in the right medial thigh and right vastus lateralis had not changed significantly. For definitive diagnosis, a punch biopsy at the right medial thigh revealed 3 sparganum measuring 5 cm in length. The histopathologic examination showed dermal and subcutaneous inflammatory infiltrates including eosinophils and sparganum larva. The larva had a thick eosinophilic microvillous tegument, with bundles of longitudinal muscle fibers scattered throughout the mesenchyme and calcospherules (Fig. 3). The patient had no history of ingesting raw snakes or frogs or of drinking unpurified water. Because the lesions were multifocal, it was impossible to completely remove the sparganum. He was administered praziquantel 100 mg/kg for 2 days.

Two months later, 6 cycles of chemotherapy were administered, and follow-up PET-CT indicated migration of the hypermetabolic lesions. A new lesion had developed in the right rectus abdominis muscle, and previous lesions in the left rectus abdominis and right buttock had disappeared (Fig. 4A, B). Nine

months later, follow-up abdomen CT showed a new peripherally enhancing tubular lesion in the left psoas muscle (Fig. 4C).

The patient was subsequently referred to another hospital for further treatment.

DISCUSSION

Sparganosis presents most commonly as fixed or migratory subcutaneous or intramuscular masses with or without tenderness. However, it also can involve internal organs such as the eyes, pleura, genitourinary tract, intestine, brain, and spinal cord. Clinically, it can mimic a neoplasm or metastasis in cancer patients and as such, initial diagnosis in most cases is very difficult. In particular, it is difficult to differentiate sparganosis from skin or subcutaneous involvement of lymphoma in lymphoma patients with multifocal sparganosis, as in our case. Imaging finding of sparganosis in lymphoma patient has rarely been reported. Roh et al. (2) reported a case of sparganosis presenting as subcutaneous masses in the chest and abdomen of a lymphoma patient whose immune system had been suppressed by chemotherapy. Lee and Yoo (3) reported axillary sparganosis misdiagnosed as lymph node metastasis in a breast cancer patient

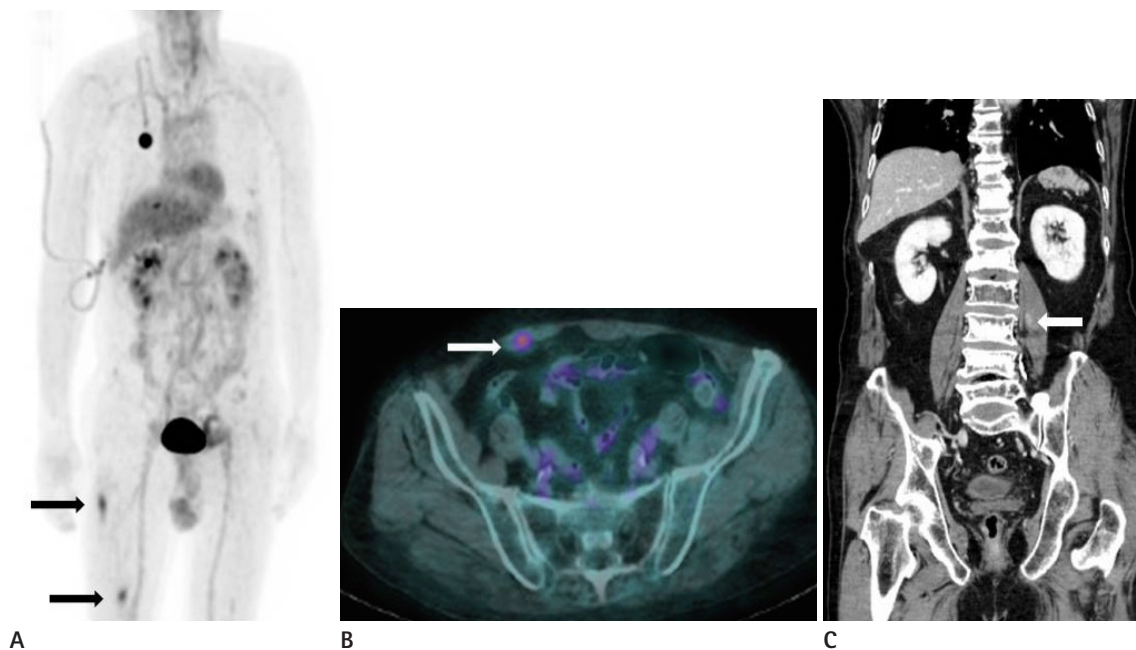


Fig. 4. Follow-up PET-CT after 2 months and abdomen CT after 9 months.

A, B. On PET-CT, a hypermetabolic tubular lesion in right buttock has disappeared, but the other lesions in right lateral thigh (**A**, black arrows) still remains (**A**) and a hypermetabolic lesion has newly developed in the right rectus abdominis muscle (**B**, white arrow).

C. Abdomen CT shows a new peripherally enhancing tubular lesion in the left psoas muscle (white arrow).

CT = computed tomography, PET-CT = positron emission tomography-computed tomography

undergoing neoadjuvant chemotherapy. Sparganosis can potentially occur independently of anticancer therapy, but philological reviews suggested that anticancer therapy induced immunosuppression might affect the pathogenesis or course of parasitic disease such as sparganosis (2). In fact, the sparganosis of our patient was detected in the course of chemotherapy.

Various radiologic evaluations are also helpful for diagnosis. Our case was the first report of multimodal US, CT, MRI, PET-CT and follow-up imaging findings to diagnose multifocal sparganosis in a patient with lymphoma. In a previous report, multiple calcifications seen on plain radiographs were interpreted as sparganum pathways (4). We found no visible calcifications on plain radiograph of our patient, but the histologic result of US-guided biopsy showed calcified materials. US is highly effective for differential diagnosis of sparganosis from superficial varicose veins or soft tissue tumor. US findings on sparganosis generally include low echogenic tubular lesion (from the sparganum itself) along with increased echogenicity of the surrounding tissue (from chronic granulomatous inflammation) (5). Previously reported MRI findings of multiple elongated tubular tracts have included low signal intensity on T1-weighted images with peripheral enhancement, and heterogeneous high signal intensity on T2-weighted images (4). The US or MRI finding of sparganosis may be similar to those of lymphoma. However, US reveals homogeneous hyperechoic thickening of the subcutaneous fat layer without internal tubular tract; and MRI shows mild heterogeneous enhancement, not rim enhancement, especially in case of subcutaneous panniculitis-like T-cell lymphoma (6, 7). In cases of cerebral sparganosis, bead-like enhancement or ring enhancement has been reported on CT (8). Lee and Yoo (3) reported axillary sparganosis with hypermetabolic activity (SUV-max 7.2) based on fluorodeoxyglucose (FDG)-PET. On PET-CT, because inflammatory processes as well as malignancy can cause increased FDG uptake, parasitic infection is often misdiagnosed as cancer. In fact, the present case showed multiple hypermetabolic lesions on PET-CT that were initially confused with lymphoma involvement. However, US, CT, MR, and PET-CT findings were retrospectively consistent with sparganosis.

A definite diagnosis of sparganosis entails detection of its larva in a wound or operative field. Sparganosis may be diagnosed using clinical symptoms, and eosinophilia and/or increase in serum IgE antibody are frequently seen. In case of worm necrosis

or impossible extirpation, enzyme-linked immunosorbent assay is effective for detection of increased IgG antibody titer. In the present case, however, the laboratory findings on the blood did not show typical eosinophilia or positivity for the IgG antibody of sparganum. Confirmation of sparganosis was made by punch biopsy of right medial thigh.

Direct removal of plerocercoids by surgical methods is the treatment of choice. Alternatively, oral administration of praziquantel or mebendazol, direct injection of procaine and 40% ethyl alcohol into the lesion, as well as venous injection of novarsenobenzol have been reported (9).

In this report, we described the multimodal US, CT, MRI, PET-CT and follow-up imaging findings on disseminated sparganosis in a patient with lymphoma. Initial diagnosis as neoplasm can lead to unnecessary interventions including invasive procedures. Familiarity with multimodal imaging findings on sparganosis can facilitate early diagnosis and subsequent clinical management.

REFERENCES

1. Lee BJ, Ahn SK, Kim SC, Lee SH. Clinical and histopathologic study of sparganosis. *Korean J Dermatol* 1992;30:168-174
2. Roh SY, Lee JY, Park KW, Jung SN. Sparganosis in a patient with diffuse large B cell lymphoma. *J Cancer Res Ther* 2013;9:712-714
3. Lee EK, Yoo YB. Axillary sparganosis which was misunderstood lymph node metastasis during neoadjuvant chemotherapy in a breast cancer patient. *Ann Surg Treat Res* 2014;87:336-339
4. Kim JI, Kim TW, Hong SM, Moon TY, Lee IS, Choi KU, et al. Intramuscular sparganosis in the gastrocnemius muscle: a case report. *Korean J Parasitol* 2014;52:69-73
5. Park HJ, Park NH, Lee EJ, Park CS, Lee SM, Park SI. Ultrasonographic Findings of Subcutaneous and Muscular Sparganosis. *J Korean Soc Radiol* 2009;61:183-187
6. Hung GD, Chen YH, Chen DY, Lan JL. Subcutaneous panniculitis-like T-cell lymphoma presenting with hemophagocytic lymphohistiocytosis and skin lesions with characteristic high-resolution ultrasonographic findings. *Clin Rheumatol* 2007;26:775-778

7. Kim YH, Kim HS, Kim SY, Hwang YJ, Seo JW, Lee JY, et al. MR findings of subcutaneous panniculitis-like T-cell lymphoma: a case report. *J Korean Radiol Soc* 2007;57:479-482
8. Song T, Wang WS, Zhou BR, Mai WW, Li ZZ, Guo HC, et al. CT and MR characteristics of cerebral sparganosis. *AJNR* 2007;28:1700-1705
9. Tsai MD, Chang CN, Ho YS, Wang AD. Cerebral sparganosis diagnosed and treated with stereotactic techniques. Report of two cases. *J Neurosurg* 1993;78:129-132

림프종으로 오인된 다발성 스파르가눔증: 초음파, 전산화단층촬영, 자기공명영상, 양전자단층촬영의 다양한 영상 소견

허소영¹ · 박지연^{1*} · 박노혁¹ · 박찬섭¹ · 권태정² · 이성윤³ · 전현정⁴

스파르가눔증은 스피로메트라 아속의 유충이 이동하여 생기는 드문 기생충 질환이다. 가장 흔한 임상양상은 종양과 유사한 피하결절이다. 저자들은 림프종 환자에서, 림프종으로 오인되었던 다발성 스파르가눔증의 초음파, 전산화단층촬영, 자기공명영상, 양전자단층촬영 및 추적검사의 다양한 영상 소견을 보고한다.

서남대학교 의과대학 명지병원 ¹영상의학과, ²병리과, ³인제대학교 일산백병원 혈액종양내과, ⁴서울의료원 혈액종양내과